

Phase Derivative Approach for Nonlinear Power Amplifier Forward Modeling with 2-D LUTs

Vesa Lampu, Lauri Anttila, Mikko Valkama

Department of Electrical Engineering, Tampere University, Finland

vesa.lampu@tuni.fi

Abstract— In this paper, we propose a new 2-dimensional (2-D) lookup table (LUT)-based scheme with spline interpolation for the modeling of wideband and heavily nonlinear power amplifiers (PAs). The spline-interpolated LUT offers a computationally light yet accurate formulation for the nonlinear characteristics, and, unlike previous such models, we incorporate the phase change information into the modeling, in addition to the traditional signal envelope. RF measurements conducted with contemporary PA systems at 3.5 GHz indicate a clear benefit in including the phase information to the algorithm. Specifically, above 2 dB improved normalized mean squared error (NMSE) and above 3 dB improved adjacent channel error power ratio (ACEPR) are obtained compared to a LUT model without the phase derivative. Moreover, it is shown that the proposed model can outperform the traditional polynomial models with much reduced computational load.

Keywords— lookup table (LUT), modeling, nonlinear, power amplifier (PA), spline interpolation.

I. INTRODUCTION

Accurate modeling of power amplifiers (PAs) is at the heart of digital predistortion (DPD) techniques, which aim to linearize the PA output [1], [2], [3], [4], [5], [6], [7], [8]. DPD greatly enhances the energy efficiency of the PA and diminishes the out-of-band (OOB) emissions of the device, allowing for tighter spectral allocation of communication channels. While such models aim for high modeling accuracy, it is simultaneously imperative that these models function as efficiently as possible, to allow for low latency and minimize the energy consumption. Computationally efficient and accurate PA models are thus in high demand in the RF community.

It is well known that the nonlinear response of a PA is dependent on the amplitude, i.e., the envelope of the input baseband signal, with models such as the (generalized) memory polynomial (MP/GMP) [1], [2], [3], [4], decomposed vector rotation (DVR)-based models [9], [10] and various lookup table (LUT)-based techniques [5], [6], [7], [8] leveraging this. This type of modeling builds on the amplitude-dependent characteristics of the PAs, however, the Volterra model indicates that the nonlinear response also has phase change (i.e., derivative)-dependent characteristics, which are taken into account e.g., in [11], [12]. Yet, to the best of the authors' knowledge, there are currently no works where the phase derivative is leveraged in LUT-based nonlinear models. Such LUT-based models have generally been shown to reduce the computational load in modeling and identification significantly compared to polynomial-based approaches [6], [7].

To this end, this paper proposes a novel, simple, yet powerful 2-dimensional (2-D) LUT technique for the modeling

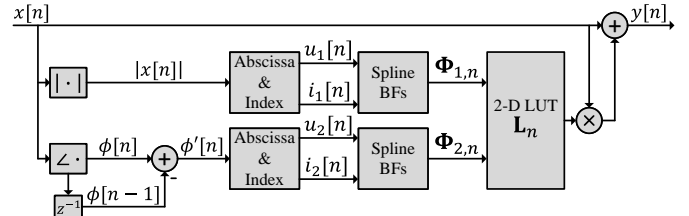


Fig. 1. The proposed 2-D LUT scheme leveraging the envelope and the phase derivative signals.

of heavily nonlinear PAs, where the phase derivative is included in addition to the amplitude in the processing system. The use of 2-D LUTs in previous works has been based on different signals in concurrent dual-band systems, e.g., in [13], [14], the average power of the input signal [15], or using the real and imaginary parts of the input signal separately [16]. Paired with spline interpolation, our RF measurements conducted with contemporary C-band PAs show that the proposed method employed in a GMP-like structure can achieve up to 2 dB improvement in modeling accuracy compared to a similar model without the phase change information. In addition, it is demonstrated that the proposed 2-D modeling can outperform polynomial-based reference models (MP, GMP), and also the simplified Volterra dynamic deviation reduction (V-DDR) [17] reference method, with much reduced computational complexity.

II. PROPOSED 2-D LUT MODELING METHOD

A. Proposed Model

To capture both the amplitude- and phase change-dependent characteristics of a nonlinear PA, let us write the baseband model for the PA output signal $y[n]$ generally as

$$y[n] = x[n]F(|x[n]|, \phi'[n]), \quad (1)$$

where $x[n]$ is the baseband PA input signal, $F(\cdot)$ is a bivariate, real-to-complex mapping function, and $\phi'[n]$ is the phase derivative signal of $x[n]$. In this work, we adopt a simple first order approximation for the phase derivative, given as $\phi'[n] = \text{mod}(\phi[n] - \phi[n-1], 2\pi)$, where $\phi[n]$ is the (unwrapped) instantaneous phase of the input signal $x[n]$. We then propose to replace $F(\cdot)$ with an $L_a \times L_p$ sized spline-interpolated LUT $\mathbf{L}_n \in \mathbb{C}^{L_a \times L_p}$. The modeling based on the 2-D LUT is shown in Fig. 1. The 2-D LUT is indexed then based on the input envelope and phase derivative as

$$y[n] = x[n] + x[n]\Phi_{1,n}^T \mathbf{L}_n \Phi_{2,n}, \quad (2)$$

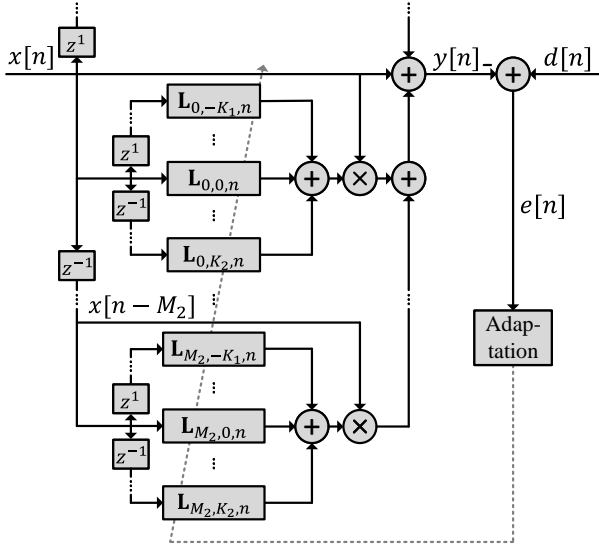


Fig. 2. Block diagram presentation of considered GMP-like LUT system.

where the LUT gain is defined to deviate from unity for improved performance in limited precision implementations and in cascaded models [7]. $\Phi_{1,n} \in \mathbb{R}^{L_a \times 1}$ and $\Phi_{2,n} \in \mathbb{R}^{L_p \times 1}$ are given as

$$\Phi_{k,n} = [0 \cdots 0 \mathbf{u}_{k,n} \mathbf{C}_P 0 \cdots 0]^T, \quad (3)$$

for $k = 1, 2$. The matrix $\mathbf{C}_P \in \mathbb{R}^{(P+1) \times (P+1)}$ is the spline basis matrix, defined separately for each interpolation order P , and the vector $\mathbf{u}_{k,n} \in \mathbb{R}^{1 \times (P+1)}$ for $k = 1, 2$ is given as

$$\mathbf{u}_{k,n} = [u_k[n]^P \ u_k[n]^{P-1} \ \cdots \ 1]. \quad (4)$$

Since the vectors $\Phi_{1,n}$ and $\Phi_{2,n}$ index the LUT based on the amplitude and phase derivative, respectively, the abscissa values $u_k[n]$ for $k = 1, 2$ are given as

$$\begin{aligned} u_1[n] &= |x[n]| - (i_1[n] - 1), \quad \text{and} \\ u_2[n] &= \phi'[n] - (i_2[n] - 1), \end{aligned} \quad (5)$$

where unit spaced LUT entries are assumed, and the indices $i_k[n]$ are given as

$$\begin{aligned} i_1[n] &= \lfloor |x[n]| \rfloor + 1, \quad \text{and} \\ i_2[n] &= \lfloor \phi'[n] \rfloor + 1. \end{aligned} \quad (6)$$

Moreover, the first non-zero elements of $\Phi_{1,n}$ and $\Phi_{2,n}$ in (3) are indexed at $i_1[n]$ and $i_2[n]$, respectively.

The update of the coefficients of the LUTs is based on the gradient-descent method, where the updates are applied towards the negative direction of the gradient of the cost function $J[n] = |e[n]|^2$ [18], with $e[n]$ being the error signal, defined as $e[n] = y[n] - d[n]$, where $y[n]$ is the model output and $d[n]$ is the measured PA response. Building on the gradient-descent fundamentals in [18], the parameter learning rule for the entries in \mathbf{L}_n can be derived and stated as

$$\begin{aligned} \mathbf{L}_{n+1} &= \mathbf{L}_n - \mu \frac{\partial J[n]}{\partial \mathbf{L}_n^*} \\ &= \mathbf{L}_n + \mu e[n] x^*[n] \Phi_{1,n} \Phi_{2,n}^T, \end{aligned} \quad (7)$$

where μ is the learning rate of the algorithm.

B. Application to GMP-like Structure

The proposed 2-D LUT scheme is next applied as a part of a GMP-like structure, shown in Fig. 2. Formally, the model is expressed as

$$\begin{aligned} y[n] &= x[n] \\ &+ \sum_{m=-M_1}^{M_2} x[n-M] \sum_{k=-K_1}^{K_2} \Phi_{1,n-m-k}^T \mathbf{L}_{m,k,n} \Phi_{2,n-m-k}, \end{aligned} \quad (8)$$

where M_1 and M_2 are the pre- and post-cursor taps, respectively, and K_1 and K_2 denote the envelope lead and lag, respectively. In addition, let us denote the total memory as $M = M_1 + M_2 + 1$, and the total envelope lag/lead as $K = K_1 + K_2 + 1$. Each memory branch in the proposed model incorporates a dedicated 2-D LUT, and the spline BF vectors $\Phi_{1,n}$ and $\Phi_{2,n}$ are computed separately for each branch. Each LUT still employs the learning rule similar to that shown in (7), since the LUTs are parallel to each other.

The computational complexity associated with the proposed GMP-like 2-D LUT model is presented in Table 1 in terms of floating point operations (FLOPs) per processed sample. It is assumed that a multiplication between complex values takes 6 FLOPs, and that delayed versions of values are stored in memory. For a hardware efficient calculation of the magnitude and phase derivative required by the 2-D LUT model, the coordinate rotation digital computer (CORDIC) algorithms can be used, which produce accurate results but add delay. If low delay is sought, more approximate models can be used at the expense of slightly higher computational complexity and lowered accuracy. For the magnitude, one such algorithm is the alpha max plus beta min algorithm, which requires 3 FLOPs to execute [19]. The phase change on the other hand can be calculated as $\phi'[n] = \arg(x[n]x^*[n-1])$, where $\arg(\cdot)$ denotes the phase of the complex argument. The inverse tangent needed for $\arg(\cdot)$ can be determined by the four quadrant version of

$$\tan^{-1}(z[n]) \approx \frac{\pi}{4} z[n] + 0.273 z[n](1 - |z[n]|), \quad (9)$$

where $z[n] = \mathcal{I}\{x[n]\} / \mathcal{R}\{x[n]\}$, which can be found in [20]. This way, the calculation of the phase derivative requires 10 FLOPs. Table 1 assumes the use of these approximate formulas.

As reference, Table 1 shows also the complexities of R -th order MP and GMP [3] and a simplified V-DDR [17] polynomial models employing similar gradient descent-based learning as the proposed model. The polynomial models incorporate self-orthogonalization to speed up and stabilize the convergence, which is carried out by adding a multiplication with a precomputed inverted autocorrelation matrix of the utilized basis function vector [18]. In Table 1, C refers to the number of basis functions in the polynomial models, which for the GMP and V-DDR models are given respectively as

$$C_{\text{GMP}} = MK \frac{R-1}{2} + M, \quad \text{and} \quad (10)$$

$$C_{\text{V-DDR}} = M(2R-1) + \frac{3}{2}(1-R). \quad (11)$$

Table 1. Computational complexities of the models in FLOPs per processed sample.

Operation	Complexity (FLOPs/sample)		
	GMP [3]	Simplified V-DDR [17]	2-D LUT (This work)
Main Path	$(K + \frac{1}{2})R - K + 8C_{\text{GMP}} - \frac{1}{2}$	$\frac{1}{2}R + 20M + 8C_{\text{V-DDR}} + \frac{23}{2}$	$4P^2 + 8P + MK(4P^2 + 10P + 5) + 6M + 17$
Learning	$8C_{\text{GMP}}^2 + 6C_{\text{GMP}} + 2$	$8C_{\text{V-DDR}}^2 + 6C_{\text{V-DDR}} + 2$	$(P + 1)^2 + MK(4(P + 1)^2) + 6M + 2$

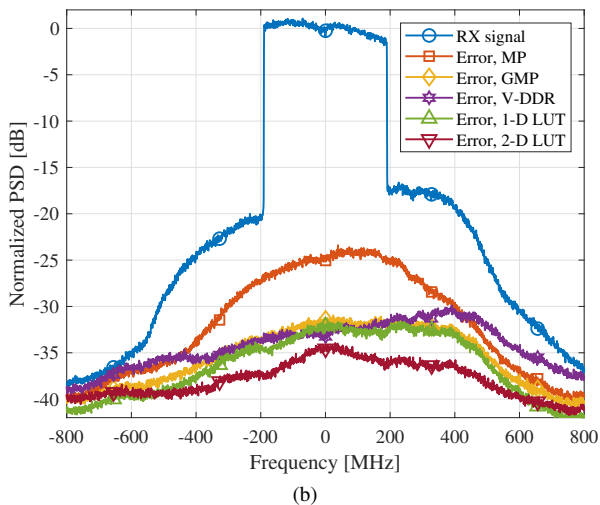
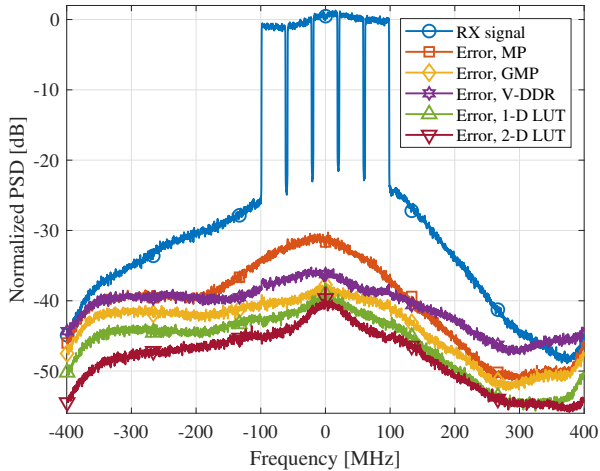


Fig. 3. Power spectral densities (PSDs) of forward modeling errors with different methods and with (a) Qorvo QPA3503; (b) NXP A5M36TG140, operating at 3.5 GHz.

III. EXPERIMENTAL RESULTS

The modeling capabilities of the proposed GMP-like 2-D LUT model and various reference models are next tested with two contemporary PAs, namely a Qorvo QPA3503 and an NXP A5M36TG140, operating on the C-band at 3.5 GHz. The PAs are excited using cyclic prefix orthogonal frequency division multiplexing (CP-OFDM) signals, the QPA3503 with a 200 MHz bandwidth (BW) signal and the A5M36TG140 with a 400 MHz BW signal, both of which have a peak-to-average power ratio (PAPR) of 7 dB. The signals are oversampled by a factor of 4, and are transmitted from a National Instruments

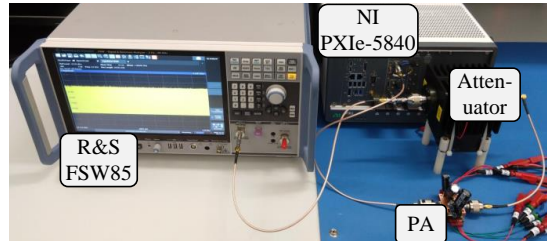


Fig. 4. RF measurement setup at 3.5 GHz illustrating the system's main parts.

Table 2. Performance metrics of the proposed 2-D LUT model and reference models with gradient descent learning. The complexity contains both the main path and learning.

Model	Complexity [FLOPs]	Memory [Real coeffs]	NMSE [dB]		ACEPR [dB]	
			Qorvo	NXP	Qorvo	NXP
MP [3]	49,781	6,240	-30.6	-22.7	-37.6	-28.8
GMP [3]	918,741	114,920	-35.8	-28.2	-41.2	-33.1
Simplified V-DDR [17]	536,403	67,080	-33.3	-27.3	-39.0	-31.4
1-D LUT ($L_p = 1$)	2,972	1,430	-37.9	-29.0	-43.5	-33.6
2-D LUT (This work)	5,221	15,730	-39.8	-31.2	-45.9	-37.0

PXIe-5840 vector signal transceiver's (VST) transmitter. The PA output is connected through an attenuator back to an RF receiver (RX) of the VST when QPA3503 is employed and—due to limited BW in the VST RX—to a Rohde & Schwarz FSW85 spectrum analyzer when employing the A5M36TG140. The measurement setup is shown in Fig. 4. In the experiments, the following parametrization is adopted for the models: $M_1 = 4$, $M_2 = 8$, $K_1 = K_2 = 2$, $P = 2$, $L_a = L_p = 11$ (in 1-D LUT, $L_p = 1$) and $R = 11$.

The power spectral densities (PSDs) of the model errors for the reference GMP model, an MP model with $K = 1$, a reference simplified V-DDR model, a reference 1-D LUT method—where the dimension L_p is set to one—and the proposed 2-D LUT method are shown in Fig. 3. The normalized mean squared error (NMSE), adjacent channel error power ratio (ACEPR) [21] for both PA measurements as well as the total number of FLOPs and required number of real-valued coefficients stored in memory in each model are gathered in Table 2. The precomputed inverted autocorrelation matrices in the polynomial models are assumed to require C^2 real-valued parameters to be stored. It is discernible from both Fig. 3 and Table 2 that the proposed 2-D LUT model is capable of outperforming all of the reference methods. In both PA measurements, the proposed 2-D LUT method achieves some 3–4 dB improved NMSE and ACEPR over the polynomial GMP model, which is the best performing of the polynomial

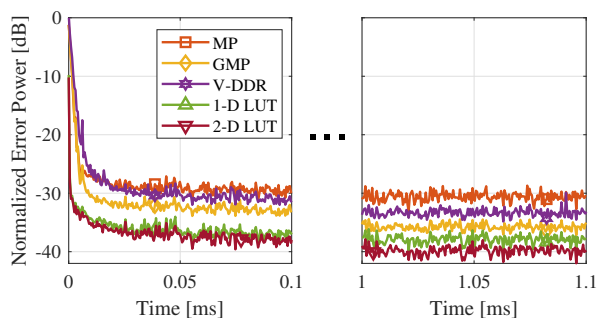


Fig. 5. Convergence of the models with Qorvo QPA3503.

models. Moreover, the benefit of adding the phase change information is evidenced, as the 2-D LUT method outperforms the 1-D LUT model without phase information by around 2 dB in NMSE and by 2–3 dB in ACEPR. The MP and simplified V-DDR models seem to suffer from the lack of information about the leading/lagging envelope, as they perform some 3 dB and 2 dB worse, respectively, than the polynomial GMP model. For reference, we note that by using least squares (LS) batch estimation, the polynomial models can achieve up to 2 dB improvement in performance with QPA3503, and up to 1 dB when the A5M36TG140 is employed. Even so, the GMP model performs on par with the 1-D LUT model, as can be expected, however, the proposed 2-D LUT model is still superior in its modeling accuracy by a 2–3 dB margin. Finally, Fig. 5 shows the convergence of the models when the QPA3503 PA is utilized. The initial drop to near –30 dB level happens almost instantaneously in all the models, while the full convergence occurs within 1 ms or so.

IV. CONCLUSION

We have proposed a novel scheme to model nonlinear PAs, leveraging both the amplitude and phase derivative information in a 2-D LUT structure, and derived the gradient-based learning rule for the LUTs. Moreover, a GMP-like model comprising of the proposed 2-D LUTs was introduced. The provided RF measurement results at 3.5 GHz utilizing modulation bandwidths up to 400 MHz, accompanied with the computational complexity assessment, revealed that the proposed 2-D LUT GMP-like model can outperform all the reference polynomial models, with much reduced computational effort. The feeding of the phase change information to the LUT was demonstrated to improve the modeling accuracy in terms of NMSE by some 2 dB, and the ACEPR by more than 3 dB compared to a traditional 1-D LUT approach.

ACKNOWLEDGMENT

This work has been supported by the Research Council of Finland under grants #332361, #338224, #345654 and by Business Finland (6GTNF project).

REFERENCES

[1] L. Ding, G. Zhou, D. Morgan, Z. Ma, J. Kenney, J. Kim, and C. Giardina, “A robust digital baseband predistorter constructed using memory polynomials,” *IEEE Transactions on Communications*, vol. 52, no. 1, pp. 159–165, 2004.

[2] O. Hammi, F. M. Ghannouchi, and B. Vassilakis, “A Compact Envelope-Memory Polynomial for RF Transmitters Modeling With Application to Baseband and RF-Digital Predistortion,” *IEEE Microwave and Wireless Components Letters*, vol. 18, no. 5, pp. 359–361, 2008.

[3] D. Morgan, Z. Ma, J. Kim, M. Zierdt, and J. Pastalan, “A Generalized Memory Polynomial Model for Digital Predistortion of RF Power Amplifiers,” *IEEE Transactions on Signal Processing*, vol. 54, no. 10, pp. 3852–3860, 2006.

[4] F. Mkadem, A. Islam, and S. Boumaiza, “Multi-Band Complexity-Reduced Generalized-Memory-Polynomial Power-Amplifier Digital Predistortion,” *IEEE Transactions on Microwave Theory and Techniques*, vol. 64, no. 6, pp. 1763–1774, 2016.

[5] K.-F. Liang, J.-H. Chen, and Y.-J. E. Chen, “A Quadratic-Interpolated LUT-Based Digital Predistortion Technique for Cellular Power Amplifiers,” *IEEE Transactions on Circuits and Systems II: Express Briefs*, vol. 61, no. 3, pp. 133–137, 2014.

[6] A. Molina, K. Rajamani, and K. Azadet, “Digital Predistortion Using Lookup Tables With Linear Interpolation and Extrapolation: Direct Least Squares Coefficient Adaptation,” *IEEE Transactions on Microwave Theory and Techniques*, vol. 65, no. 3, pp. 980–987, 2017.

[7] P. Pascual Campo, L. Anttila, D. Korpi, and M. Valkama, “Cascaded Spline-Based Models for Complex Nonlinear Systems: Methods and Applications,” *IEEE Transactions on Signal Processing*, vol. 69, pp. 370–384, 2021.

[8] L. Sun, X. Hu, Z. Liu, K. Han, S. Zhang, W. Wang, and F. M. Ghannouchi, “A Low Complexity LUT-Based Digital Predistortion Block With New Pruning Method,” *IEEE Microwave and Wireless Components Letters*, vol. 32, no. 9, pp. 1131–1134, 2022.

[9] A. Zhu, “Decomposed Vector Rotation-Based Behavioral Modeling for Digital Predistortion of RF Power Amplifiers,” *IEEE Transactions on Microwave Theory and Techniques*, vol. 63, no. 2, pp. 737–744, 2015.

[10] W. Cao and A. Zhu, “A Modified Decomposed Vector Rotation-Based Behavioral Model With Efficient Hardware Implementation for Digital Predistortion of RF Power Amplifiers,” *IEEE Transactions on Microwave Theory and Techniques*, vol. 65, no. 7, pp. 2443–2452, 2017.

[11] E. G. Lima, T. R. Cunha, and J. C. Pedro, “A Physically Meaningful Neural Network Behavioral Model for Wireless Transmitters Exhibiting PM-AM/PM-PM Distortions,” *IEEE Transactions on Microwave Theory and Techniques*, vol. 59, no. 12, pp. 3512–3521, 2011.

[12] A. Zhu, J. C. Pedro, and T. J. Brazil, “Dynamic Deviation Reduction-Based Volterra Behavioral Modeling of RF Power Amplifiers,” *IEEE Transactions on Microwave Theory and Techniques*, vol. 54, no. 12, pp. 4323–4332, 2006.

[13] A. Molina, K. Rajamani, and K. Azadet, “Concurrent Dual-Band Digital Predistortion Using 2-D Lookup Tables With Bilinear Interpolation and Extrapolation: Direct Least Squares Coefficient Adaptation,” *IEEE Transactions on Microwave Theory and Techniques*, vol. 65, no. 4, pp. 1381–1393, 2017.

[14] N. Naraharisetti, P. Roblin, C. Quindroit, and S. Gheitanchi, “Efficient Least-Squares 2-D-Cubic Spline for Concurrent Dual-Band Systems,” *IEEE Transactions on Microwave Theory and Techniques*, vol. 63, no. 7, pp. 2199–2210, 2015.

[15] J. Swaminathan and P. Kumar, “Design of efficient adaptive predistorter for nonlinear high power amplifier,” *Wireless Personal Communications*, vol. 82, pp. 1085–1093, 2015.

[16] C. Liu and H. Zhao, “A 2D-LUT Scheme Design for Complex-Valued Spline Adaptive Filter,” *IEEE Transactions on Circuits and Systems II: Express Briefs*, vol. 70, no. 8, pp. 3154–3158, 2023.

[17] L. Guan and A. Zhu, “Simplified dynamic deviation reduction-based Volterra model for Doherty power amplifiers,” in *2011 Workshop on Integrated Nonlinear Microwave and Millimetre-Wave Circuits*, 2011, pp. 1–4.

[18] S. Haykin, *Adaptive Filter Theory*, 3rd ed. Prentice Hall, 1996.

[19] R. G. Lyons, *Understanding digital signal processing, 3/E*. Pearson Education India, 1997.

[20] S. Rajan, S. Wang, R. Inkol, and A. Joyal, “Efficient approximations for the arctangent function,” *IEEE Signal Processing Magazine*, vol. 23, no. 3, pp. 108–111, 2006.

[21] A. S. Tehrani, H. Cao, S. Afsardoost, T. Eriksson, M. Isaksson, and C. Fager, “A Comparative Analysis of the Complexity/Accuracy Tradeoff in Power Amplifier Behavioral Models,” *IEEE Transactions on Microwave Theory and Techniques*, vol. 58, no. 6, pp. 1510–1520, 2010.